JOURNAL OF AIRCRAFT
Vol. 38, No. 4, July–August 2001

Experimental Investigation of Multielement Airfoil Lift Hysteresis due to Flap Rigging

Drew Landman* and Colin P. Britcher†
Old Dominion University, Norfolk, VA 23529-0247

A study is reported on a particular type of lift hysteresis discovered while developing experimental geometry optimization techniques for high-lift airfoils. A modern three-element airfoil model with a remotely actuated flap was designed, tested, and used in low-speed wind tunnel experiments to investigate optimum flap positioning based on lift. Hysteresis in lift as a function of flap position was discovered when tests were conducted using continuous flow conditions. It was shown that optimum or near-optimum lift coefficients determined using continuous flow conditions exist over an extended range of flap positions when compared to those determined using traditional intermittent conditions.

Nomenclature

C_l	=	lift coefficient, L/qc
C_p	=	pressure coefficient, $(P - P_\infty)/q_\infty$
c	=	airfoil nested chord length
L	=	lift
P	=	local static pressure
P_∞	=	freestream static pressure
q_∞	=	freestream dynamic pressure
Re_c	=	chord Reynolds number, $\rho Vc/\mu$
V	=	velocity
x	=	horizontal spatial coordinate
y	=	vertical spatial coordinate
α	=	angle of attack (referenced from nested airfoil maximum length line)
δ_{flap}	=	flap deflection angle
δ_{slat}	=	slat deflection angle
μ	=	viscosity
ρ	=	density
$\%c$	=	percent of nested chord length

Introduction

AN important practical problem in wind tunnel testing of multielement airfoils is the requirement to test a range of configurations, to ensure that the optimum is chosen.[1–7] In a companion publication, studies have described experimental geometry optimization techniques using a remotely actuated flap on a three-element airfoil, where it was shown that the time required for system optimization can be greatly reduced.[7] Flow conditions during these studies have been described as intermittent, meaning that the flow was stopped after each evaluation of lift coefficient and restarted before the next. In an effort to further expedite in situ optimization during the experimental program of Ref. 7, trials were conducted without interrupting the flow between successive lift evaluations. These studies revealed lift hysteresis as a function of flap position, which presented a multivalued problem to a simple steepest ascent optimizer, incapable of distinguishing path. The main thrust of this study is to explore the origin of this flow phenomenon and its influence on lift measurement. Additionally, it is shown that it may be possible to exploit this inherent lift hysteresis in the choice of optimal multielement rigging. The work presented in this paper represents a building block in the process of developing an automated full three-dimensional modeling approach to multielement airfoil experimental optimization at near-flight conditions.

Flow Hysteresis

Hysteretic behavior is often observed in the C_L–α curve of two-dimensional airfoils or three-dimensional wings. Perhaps the most common occurrence is hysteresis around classical stall, where the lift loss at stall is not recovered until the angle of attack is significantly reduced.[8] Low Reynolds number, airfoils frequently exhibit separation bubble induced hysteresis,[9] usually in the positive sense, that is, similar to stall hysteresis, but occasionally reversed. Changes in model geometry can induce hysteretic behavior. For example, slot lip spoilers deployed in conjuction with Fowler flaps have been shown to exhibit significant aerodynamic hysteresis in the C_L–α curve for large flap deflections where none may occur for lower flap deflection angles.[10] Hysteretic behavior is also observed with three-dimensional bluff bodies, typically including wake structure changes with varying orientation.

In all of the cases mentioned, the underlying phenomenon is interaction between the inviscid outer flowfield and the viscous boundary layer, specifically, the separation points thereof. The coupling mechanism is the separation region itself, which can substantially modify the outer flow, hence the surface pressure distribution. The majority of reported data show C_L or C_D varying as a function of orientation. Occasionally, hysteresis is observed as a function of Reynolds number at a fixed orientation. No previous published work was identified that discussed aerodynamic hysteresis based on flap position for a given angle of attack and fixed flow conditions.

Experimental Details

A unique model with internal actuators was specially designed using airfoil geometry representative of a modern civil transport.[7,11] Nomenclature for multielement airfoils is reviewed in Fig. 1. Slat deflection was fixed at 30 deg for the entire test; slat gap and overhang were varied by installing shims under brackets. Two slat settings were used: setting A had a 3.03%c gap and a −2.46%c overhang and setting B used a 2.17%c gap and a −1.46%c overhang. The flap was designed for a positional gap range of 1.38%c–4.4%c (based on the nested chord of the entire model) and an overhang range of −1.38%c–3.63%c. The flap is positioned using four servomotors located in the main element, arranged in two-degree-of-freedom stages, two motors to a stage, as shown in Fig. 2. Linear motion is provided in the horizontal direction x and vertical direction y, and flap deflection angle is fixed at 30 deg.

The Old Dominion University, Department of Aerospace Engineering, 4 × 3 ft low-speed wind tunnel was used to obtain all of the results presented. This wind tunnel is a closed return, fan driven,

Received 12 July 2000; revision received 12 February 2001; accepted for publication 17 February 2001.

*Assistant Professor, Department of Aerospace Engineering. Member AIAA.
†Associate Professor, Department of Aerospace Engineering. Senior Member AIAA.

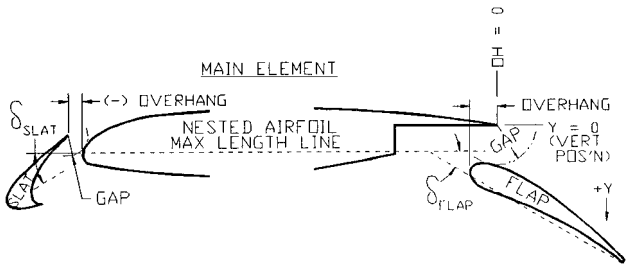

Fig. 1 Multielement airfoil nomenclature.

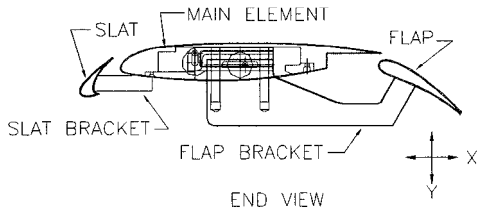

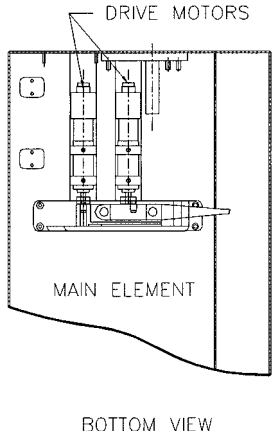

Fig. 2 Three-element airfoil wind-tunnel model.

atmospheric pressure tunnel using a 125 hp electric motor to provide speeds in excess of 120 mph. The test section is 4 × 3 ft in cross section and 8 ft long. The freestream turbulence intensity in this facility does not exceed 0.2%. Further details of the model, installation, and instrumentation are provided in Refs. 7 and 11.

A test Reynolds number of 1×10^6 was chosen based on the maximum normal force sustainable by the automated model. Initial tests in this study were conducted with free boundary-layer transition, meaning there were no added tripping devices or surface roughness elements on the airfoil. Later, roughness elements were added in an effort to force transition on the upper surface of all the elements. It was felt that the forced transition would eliminate the possibility of laminar separation bubble induced hysteretic effects.[9,12] Forcing transition is one method for simulating higher Reynolds number flows, which has the benefit of allowing comparisons to higher Reynolds number data.[13,14] A number 30 grit abrasive particle (diameter of approximately 0.028 in.) was chosen as the minimum size roughness element necessary to assure transition.[15] The particles were distributed with a 40% coverage over approximately a 0.2-in.-wide strip, whose leading edge was located at the 5% element chord location on the top surface of each element.[13,16] No differences were found in the distribution of lift vs flap position between the free and forced transition measurements; however, results are annotated to indicate which method was used.

All results are presented without corrections for boundary effects. Sample element pressure and lift distribution comparisons to reference data as well as uncertainty level analyses for lift have been presented in Ref. 7. The focus of this study was the comparative evaluation of C_l vs flap position (not to obtain C_l for this configuration with absolute accuracy). The estimated 95% confidence level of precision in C_l including the collective effect of instrumentation and positioning was found to be less than 0.5% of the measured C_l.

Lift Hysteresis Based on Flap Position: Experimental Evidence

The remotely actuated flap was used to vary flap gap and overhang both with the tunnel flow on continuously and with the flow restarted between successive data points (hereafter called intermittently). In both cases, for fixed slat riggings, excessive flap gap settings led to separation on the flap progressing from the trailing edge and moving forward as the gap was increased. This separation trend was identified by the constant pressure region at the trailing-edge flap and was verified using tufts.[8,17]

The nature of the progression of flap stall was found to be both path dependent and dependent on whether the tunnel was operated continuously or intermittently. Four paths were chosen to study stall progression and are presented in Fig. 3. Each path represents motion in one degree of freedom while the second degree of freedom is fixed, that is for example, changing vertical position with fixed overhang. The arrows show the direction in which the flap was moved. The underlying contours show the baseline distribution of airfoil lift coefficient, derived from the integrated pressure data, taken with intermittent flow conditions. Pressure distributions for the points of the intermittent flow paths in Fig. 3 are shown in Figs. 4–7; Fig. 7 represents a path that extended outside of the region where baseline data was available. The progression toward flap stall under intermittent

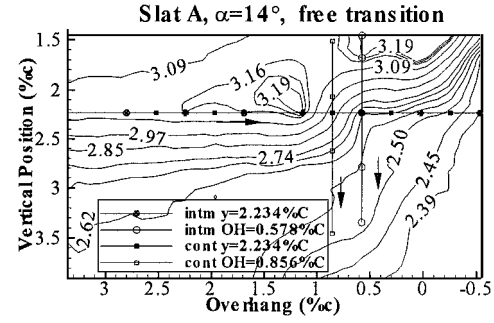

Fig. 3 Paths of the stall progression study.

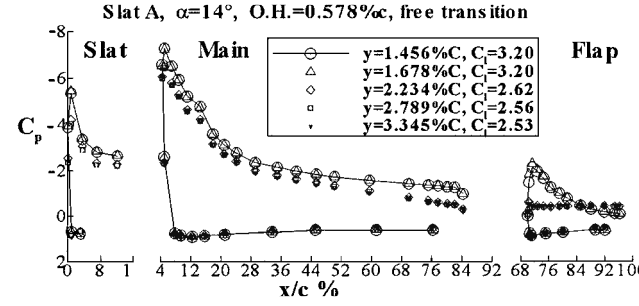

Fig. 4 Stall progression with intermittent flow conditions, overhang (OH) = 0.578%*c*.

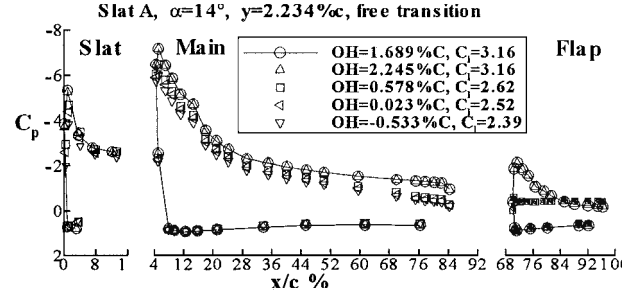

Fig. 5 Stall progression with intermittent flow conditions, *Y* = 2.234%*c*.

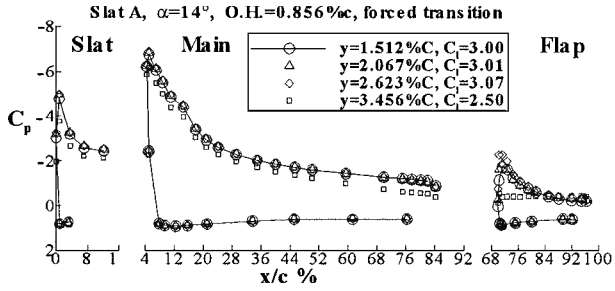

Fig. 6 Stall progression with continuous flow conditions, OH = 0.856%*c*.

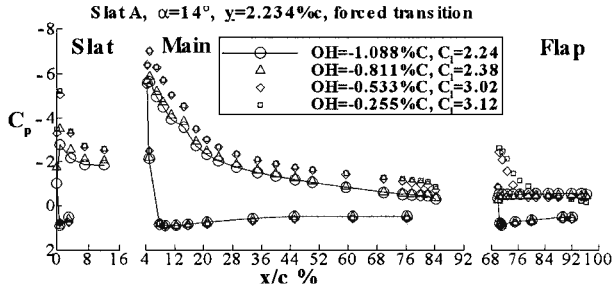

Fig. 7 Stall progression with continuous flow conditions, *Y* = 2.234%*c*.

flow conditions is seen in Fig. 4, where the flow is completely attached for $y = 1.456\%c$ and $y = 1.678\%c$ but completely separates somewhere between $y = 1.678\%c$ and $y = 2.234\%c$ as the flap is moved downward. The full separation is evidenced by the nearly constant pressure over the entire upper surface of the flap. A similar trend is observed in Fig. 5, which shows the stall progression as the flap is moved aft under intermittent conditions. The interaction of the three elements can be seen in the deleterious effect the flap has on the two upstream elements as the flap approaches stall. The decreased circulation on the flap results in a reduced upper surface suction pressure at the trailing edge of the main element, hence, a reduced circulation on the main element. The reduced circulation on the main element similarly influences the slat, Smith's circulation effect.[18] The effect of increasing gap on flap stall is shown in Fig. 5. When the flap leading edge is under the trailing edge of the main element, resulting in a relatively constant gap, pressure distributions remain nearly identical. As the flap leading edge moves toward the main element trailing edge, the airfoil lift coefficient rises with the increasing gap until a local maximum is reached, and then the flap quickly stalls with any further increase in gap.

The results presented in Figs. 4 and 5 were obtained using natural boundary-layer transition. To address the possibility of obtaining ambiguous results due to low Reynolds numbers effects, such as laminar separation bubbles, the continuous flow studies were conducted using forced transition as described earlier. When comparing forced vs free transition, a small decrease in overall lift on the order of the experimental uncertainty was the only difference observed; the onset of stall was found to exist at identical flap positions.[7] Figures 6 and 7 present the results of the continuous flow stall progression study. When comparing the intermittent and continuous stall progression results, it is evident that the stall is delayed for both the vertical and horizontal sweeps. In other words, the size of the gap for which stall occurs is comparatively larger in the continuous flow case vs the intermittent case. However, the mechanism for stall appears to remain the same. Pressure distributions again indicate that separation begins at the trailing edge of the flap and progresses forward until the flow is fully separated over the upper surface of the flap. This can be seen in Fig. 7 as the flap pressure distribution progressively flattens near the trailing edge as the flap moves from an overhang from $-0.255\%c$ to $-1.088\%c$. In comparing this sequence to Fig. 5, note that the increments in overhang are reduced, yielding greater detail such as capturing the separated flow over approximately 60% of the flap at an overhang of $-0.533\%c$.

From the stall progression study, it was noted that the flap stalled at a more aft overhang setting and with a larger gap when the flow was left on during flap movement (compare Figs. 5 and 7, for example). This finding led to an interest in identifying the shape and extent of the region of delayed stall. Initially, overhang and vertical sweeps were conducted for a 14-deg angle-of-attack case with both slat riggings, using free transition. The results of these tests are shown in Figs. 8 and 9 with the detailed swept paths from the slat A case together with the baseline values shown in Figs. 10–12. A flap movement from a condition of maximum overhang or minimum vertical distance to a condition of minimum overhang or maximum vertical distance is defined as an outgoing path, and the same path reversed in direction is defined as the return path. All sweeps were

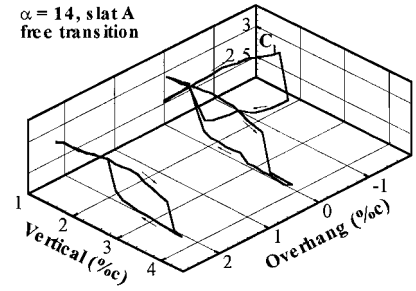

Fig. 8 Hysteresis sweep, free transition, slat A.

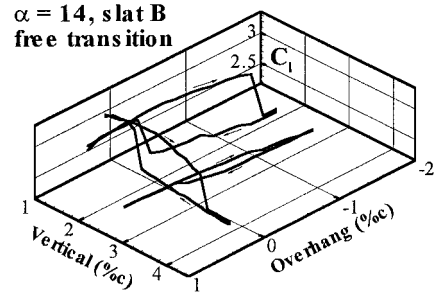

Fig. 9 Hysteresis sweep, free transition, slat B.

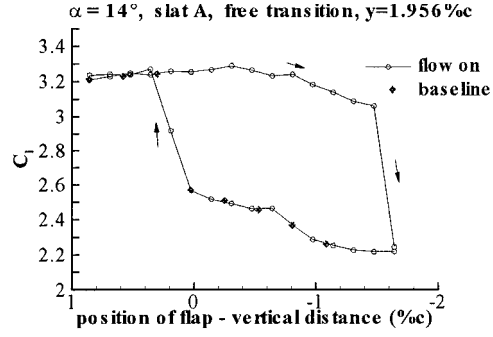

Fig. 10 Hysteresis sweep of Fig. 8 with baseline, *Y* = 1.956%*c*.

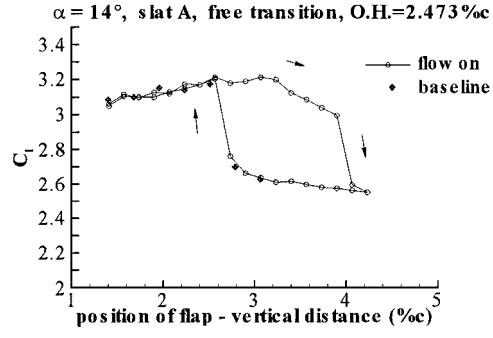

Fig. 11 Hysteresis sweep of Fig. 8 with baseline, OH = 2.473%*c*.

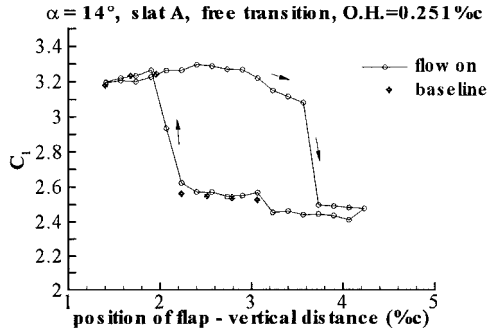

Fig. 12 Hysteresis sweep of Fig. 8 with baseline, OH = 0.251%*c*.

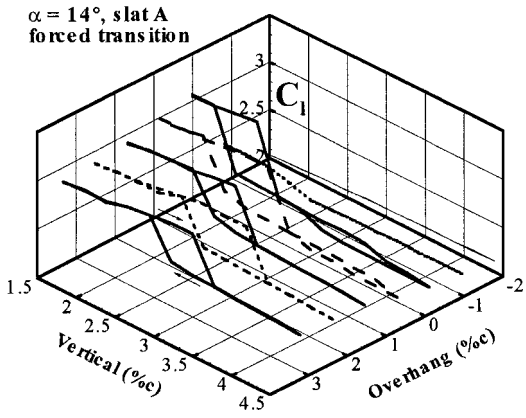

Fig. 13 Hysteresis sweep, forced transition, slat A.

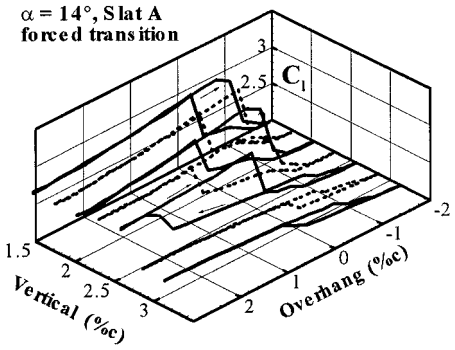

Fig. 14 Hysteresis sweep, forced transition, slat A continued.

conducted by moving the flap to the first point of the outgoing path, starting the tunnel, establishing the desired flow conditions, and then traversing the flap from point to point on the outgoing path stopping at each point to sample pressures. Then, without turning off the flow, the flap was traversed along the return path back to the start point, stopping at the same points to sample pressures. For the six runs of Figs. 8 and 9, it was found that all of the measured baseline lift coefficients (flow off between runs) coincided with the return paths. This trend was identified in all of the subsequent runs whether forced or free transition was invoked. Perhaps the most interesting and significant result of this whole study was first discovered in the data of Figs. 10–12: Following an outgoing path on either a fixed overhang or vertical path, it appears that C_l actually increases to a value beyond the maximum found by traditional methods using intermittent flow conditions. The increase is on the order of the experimental uncertainty[7]; however, this trend is repeated in the results discussed subsequently. No significant differences due to the slat riggings, that is, A vs B, were noted in the shape or extent of the hysteresis loops.

These initial results sparked an interest in a detailed study with a dense spacing of hysteresis sweeps. Forced transition was used for this study, and results are shown in Figs. 13 and 14. Figure 15 shows the available lift increment due to hysteresis. Figures 16–20

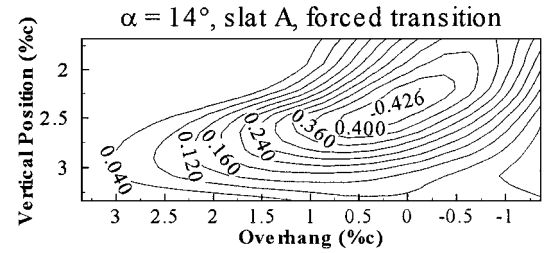

Fig. 15 Lift increment due to hysteresis.

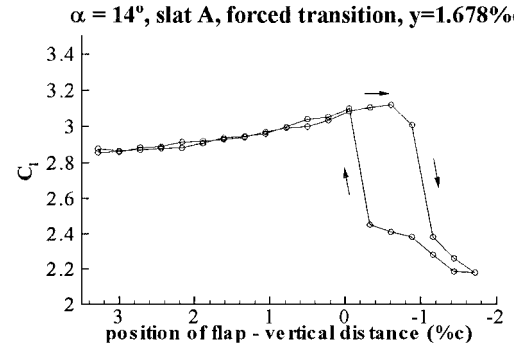

Fig. 16 Hysteresis sweep of Fig. 14, *Y* = 1.678%*c*.

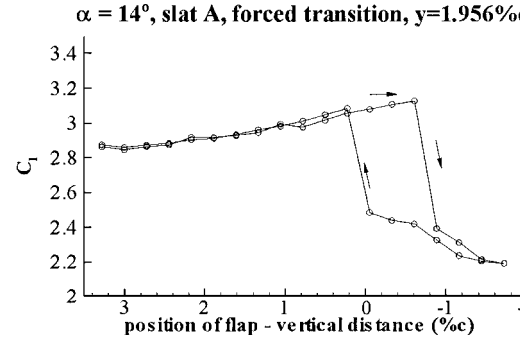

Fig. 17 Hysteresis sweep of Fig. 14, *Y* = 1.956%*c*.

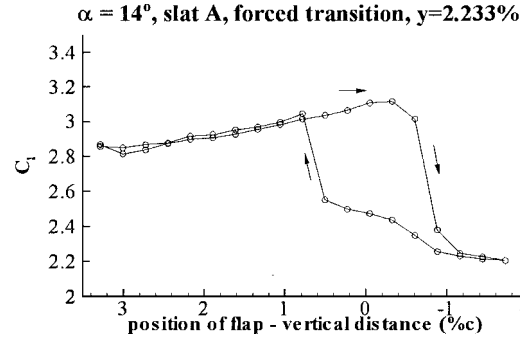

Fig. 18 Hysteresis sweep of Fig. 14, *Y* = 2.233%*c*.

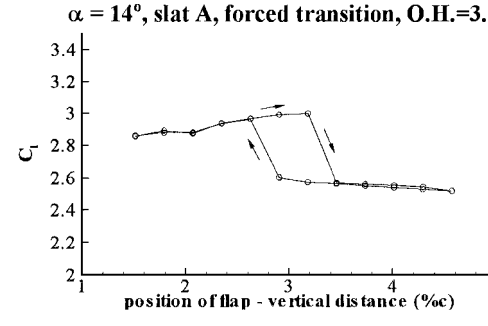

Fig. 19 Hysteresis sweep of Fig. 13, OH = 3.306%*c*.

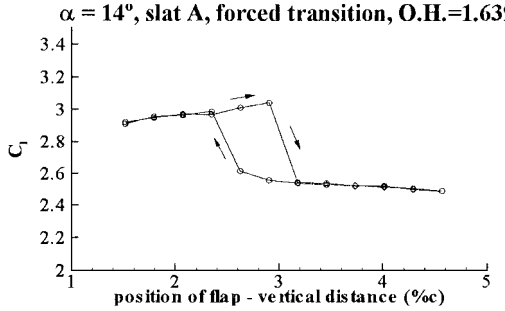

Fig. 20 Hysteresis sweep of Fig. 13, OH = 1.639%*c*.

contain details of some of the sweeps conducted in Figs. 13 and 14. Again, an outgoing sweep showed an increase in C_l beyond the value found by using intermittent methods in all of the cases where a sweep was performed starting in a region of attached flow on the flap. The vertical sweeps, which started in the region where the flap was fully stalled, did not exhibit hysteresis. A limited study was performed using an 8-deg angle of attack and the A slat rigging with free transition. The previous trend, which showed a continued increase in C_l above the intermittent baseline value, was not evident in these runs, suggesting that this phenomenon is dependent on angle of attack.

Discussion

Flow Physics of Lift Hysteresis

Multielement airfoil lift hysteresis as a function of angle of attack has been previously reported.[8] In that study, it was found that an airfoil and flap configured for high lift exhibited a hysteresis loop in the lift curve when the two-dimensional model was cycled in angle of attack from zero lift to complete stall (both elements). Several configurations, including optimal, large, and small gaps, were tested, and in each case the flap stalled first. The mechanism for stall was described in the same way as that of the element stall study of this work, namely, trailing-edge stall of the flap.

A hypothesis has been developed to describe the lift hysteresis due to flap motion. Consider an overhang sweep (vertical position constant) where the starting point is well forward (positive overhang). As the flap progresses aft, the gap is initially constant, and as a result, the pressure distribution remains relatively unchanged, as shown in Fig. 5. As the flap continues to move aft, the flap gap begins to widen, and the size and influence of the potential jet flow region increases, providing a more favorable pressure gradient over the upper surface of the flap, which promotes a thin, laminar boundary layer. The slot flow centerline tends to follow the flap curvature under the influence of the strong pressure gradients of the wing wake.[8,19–21] This beneficial interaction continues until the gap reaches a critical width, at which time the point of separation on the flap begins to move forward from the trailing edge.[22] This is understood to be a result of the now reduced jet flow velocity with its accompanying increasingly adverse pressure gradient. The separation point on the flap upper surface travels forward with increasing gap until the main element wake and flap boundary layer begin mixing.[8] As the flap is moved further aft, more turbulent mixing occurs until eventually the flap is fully stalled.[8] As the flap now begins to traverse the return path, the turbulent mixing is well established. The high momentum carried in the main element wake (including the slat wake) mixes with the lower momentum of the flap boundary layer maintaining separated flow over the flap (seen in the constant pressure distributions on the flap upper surface) until the slot flow is well established again and mixing begins to subside.

That the flap stalls at a further aft position under continuous flow conditions than under intermittent conditions can be attributed to the establishment of a favorable slot flow and flap boundary layer. When continuous conditions are used for testing, the slot flow and flap boundary layer are well established while the flap gap is small. The flap can then be moved to a position where, under intermittent testing conditions, the gap will produce a stalled flap. The intermittent conditions force the boundary layer on the flap to develop under conditions established by low Reynolds numbers, which are known to be susceptible to separation. If the flap boundary layer initially separates and begins to mix with the wake of the main element while the flow accelerates, the effects may be irreversible.

Optimization with Hysteresis Present

If wind-tunnel productivity for high-lift testing is to be maximized, optimization methods using automated models tested with continuous flow conditions represent the ultimate goal. Irreversibility in the form of lift hysteresis presents a significant challenge to optimization algorithms. Experimental evidence has shown that while traversing the flap of a three-element airfoil to achieve maximum lift, an ideal configuration often occurs just before massive flow separation on the upper surface of the flap. If the direction of the search is reversed just after the flap has stalled, the irreversible nature of the flow prevents reattachment, and the value for the lift coefficient found during the approach to the maximum is now much lower at the same point in the design space. Hence, the objective function is multivalued and path dependent.

Consider an optimizer negotiating the paths of Figs. 16–18. Moving along any of the three outgoing paths other than the $Y = 1.956\%c$ path with a small enough step size so as not to greatly overshoot the optimum should result in convergence. On the other hand, approaching the optimum of the $Y = 1.956\%c$ path (Fig. 17) is more difficult due to the sudden stall. As an alternative, intelligent algorithms could be employed, possibly using knowledge gained from an initial coarse baseline data set, which use unidirectional search patterns that retain a path history. Algorithm sensitivity to separated flow could be incorporated by monitoring top surface flap pressures, allowing identification of impending stall.

Conclusions

This study revealed an irreversible flow phenomenon that complicates in situ automated high-lift wind-tunnel model geometry optimization techniques. Whereas in situ geometry optimization of automated multielement airfoils has been shown to be practical using intermittent flow conditions, more work is required to extend this technology to include continuous flow applications. Through the development of these techniques, large wind-tunnel productivity gains are realizable. The natural extension is to now develop a three-dimensional testing pilot study at near-flight conditions, where the greatest challenge may be the mechanical design of a three-dimensional wing model capable of withstanding the high loading associated with these flow conditions. Perhaps lift hysteresis is influenced by Reynolds number, or three-dimensional effects; further study will tell.

Acknowledgments

This work was partially funded by two American Society for Engineering Education summer faculty fellowships at the NASA Langley Research Center (LaRC) with the Experimental Flow Physics Branch (EFPB) and the Subsonic Aerodynamics Branch. Additional funding was received from NASA LaRC task orders, one from EFPB and a second from the Multi-Disciplinary Design and Optimization Branch. Specifically, the authors wish to acknowledge the help of S. Robinson, M. Walsh, J. Lin, S. Klausmeyer, E. Waggoner, H. Morgan, J. Otto, F. Backley, and T. Zang.

References

[1] Butter, D. J., "Recent Progress on Development and Understanding of High Lift Systems," CP-365, AGARD, 1984.

[2] Lynch, F. T., "Experimental Necessities for Subsonic Transport Configuration Development," AIAA Paper 92-0158, Jan. 1992.

[3] Valarezo, W. O., Dominik, C. J., and McGhee, R. J., "Multielement Airfoil Performance due to Reynolds and Mach Number Variations," *Journal of Aircraft,* Vol. 30, No. 5, 1993, pp. 689–694.

[4] Klausmeyer, S. M., and Lin, J. C., "Comparative Results From a CFD Challenge over a 2D Three-Element High Lift Airfoil," NASA TM 112858, May 1997.

[5]Lin, J. C., and Dominik, C. J., "Optimization of an Advanced Design Three Element Airfoil at High Reynolds Numbers," AIAA Paper 95-1858, 1995.

[6]Valarezo, W. O., Dominik, C. J., McGhee, R. J., Goodman, W. L., and Paschal, K. B., "Multi-Element Airfoil Optimization for Maximum Lift at High Reynolds Numbers," AIAA Paper 91-3332, Sept. 1991.

[7]Landman, D., and Britcher, C. P., "Experimental Geometry Optimization Techniques for Multielement Airfoils," *Journal of Aircraft,* Vol. 37, No. 4, 2000, pp. 707–713.

[8]Biber, K., and Zumwalt, G. W., "Hysteresis Effects on Wind Tunnel Measurements of a Two-Element Airfoil," *AIAA Journal,* Vol. 31, No. 2, 1993, pp. 326–330.

[9]Selig, M. S., Guglielmo, J. J., Broeren, A. P., and Giguère, P., "Experiments on Airfoils at Low Reynolds Numbers," AIAA Paper 96-0062, Jan. 1996.

[10]Wentz, W. H., "Effectiveness of Spoilers on the GA(W)-1 Airfoil with a High Performance Fowler Flap," NASA CR-2538, May 1975.

[11]Landman, D., "Experimental Geometry Optimization Techniques for Multi-Element Airfoils," Ph. D. Dissertation, Dept. of Aerospace Engineering, Old Dominion Univ., Norfolk, VA, May 1998.

[12]Mueller, T. J., and Batill, S. M., "Experimental Studies of Separation on a Two-Dimensional Airfoil at Low Reynolds Numbers," *AIAA Journal,* Vol. 20, No. 4, 1982, pp. 457–463.

[13]Barlow, J. B., Rae, W. H., and Pope, A., *Low Speed Wind Tunnel Testing,* 3rd ed., Wiley, New York, 1999, pp. 301–320.

[14]Pankhurst, R. C., and Holder, D. W., *Wind Tunnel Technique,* rev. ed., Sir Issac Pitman and Sons, London, England, 1965.

[15]Braslow, A. E., and Knox, E. C., "Simplified Method for Determination of Critical Height of Distributed Roughness Particles for Boundary-Layer Transition at Mach Numbers from 0 to 5," NACA TN 4363, Sept. 1958.

[16]Papadakis, M., Myose, R. Y., and Matallana, S., "Experimental Investigation of Gurney Flaps on a Two Element General Aviation Airfoil," AIAA Paper 97-0728, 1997.

[17]Adair, D., and Horne, W. C., "Characteristics of Merging Shear Layers and Turbulent Wakes of a Multi-Element Airfoil," NASA TM 100053, Feb. 1988.

[18]Smith, A. M. O., "High-Lift Aerodynamics," AIAA Paper 74-939, 1974.

[19]Nelson, R. C., "An Overview of High Lift Aerodynamics," AIAA Professional Studies Series, Jan. 1995.

[20]Nakayama, A., Kreplin, H. P., and Morgan, H. L., "Experimental Investigation of Flowfield About a Multielement Airfoil," *AIAA Journal*, Vol. 28 No. 1, 1990, pp. 14–21.

[21]Olson, L. E., and Orloff, K. L., "On the Structure of Turbulent Wakes and Merging Shear Layers of Multielement Airfoils," AIAA paper 81-1248, June 1981.

[22]Brune, G. W., and McMasters, J. H., "Computational Aerodynamics Applied to High-Lift Systems," *Applied Computational Aerodynamics,* edited by P. A. Henne, Vol. 125, Progress in Astronautics and Aerononautics, AIAA, Washington, DC, 1990, pp. 389–433.